

Neryl acetate, the major component of Corsican *Helichrysum Italicum* essential oil mediates its activity

Neryl acetate increases skin barrier function

Géraldine Lemaire^{1*}, Malvina Olivero¹, Alain Moga², Aurélie Pagnon³, Virginie Rouquet¹, Valérie Cenizo¹, Pascal Portes¹

¹ Laboratoires M&L SA, Groupe L'Occitane, Manosque, France; ² QIMA Life Sciences, QIMA-Synelvia, Labège, France; ³ Novotec, Bron, France

* Géraldine Lemaire, Laboratoires M&L SA, Groupe L'Occitane, ZI St Maurice, Manosque, France, +33492702579, geraldine.lemaire@locctane.com

Background: Corsican *Helichrysum Italicum* essential oil is characterized by high concentrations of neryl acetate, and we previously demonstrated that Corsican *Helichrysum Italicum* essential oil increases the expression of genes that are part of the differentiation complex (*involucrin*, *small proline rich proteins*, *late cornified envelope*, *S100 protein family*).

Methods: The biological activities of *Helichrysum Italicum* essential oil and neryl acetate were compared to identify how neryl acetate contributes to *Helichrysum Italicum* essential oil activity on human skin. Neryl acetate, as a part component of *Helichrysum Italicum* essential oil, was tested on skin explant models for 24 hours and 5 days in comparison with *Helichrysum Italicum* essential oil. We analyzed the biological regulations in the skin explant by transcriptomic analysis, skin barrier protein immunofluorescence, lipid staining and ceramide analysis by liquid chromatography-mass spectrometry.

Results: Transcriptomic analysis revealed that 41.5% of *Helichrysum Italicum* essential oil-modulated genes were also regulated by neryl acetate and a selected panel of genes were confirmed by quantitative reverse transcription PCR analysis. Those genes are involved in epidermal differentiation, skin barrier formation and ceramide synthesis. Involucrin, involved in formation of the cornified envelope, was upregulated at both gene and protein levels after 24 hours and 5 days respectively. After 5 days of treatment, total lipids and ceramides were also increased.

Conclusion: Our results demonstrate that neryl acetate mediates a large part of Corsican *Helichrysum Italicum* essential oil activity on skin barrier formation.

Keywords: *Helichrysum italicum*, Neryl acetate, skin barrier formation, ceramides

Introduction

Helichrysum Italicum (Roth) G. Don subsp. *Italicum* from the *Asteraceae* family grows on dry, rocky or sandy ground around the Mediterranean Basin and is commonly known as the everlasting plant [1]. *Helichrysum Italicum* essential oil (HIEO) is obtained from the hydrodistillation of aerial parts [2] and its composition is known to depend on the geographical area of collection [3, 4]. Indeed, the chemical composition of the HIEOs collected in Sicily and Corsica analyzed by Schipilliti *et al.* [5] shows that Sicilian oils are rich in α - and β -selinene, rosifoliol and aromadendrene, whereas Corsican oils are rich in neryl acetate (NA), α -pinene and γ -curcumene. The highest NA content found in Corsican HIEO from plants collected in the flowering stage is correlated with relatively weak soil acidity and low percentages of clay, fine sand and coarse silt and with high percentages of coarse sand and fine silt [6].

NA is an acetate ester resulting from formal condensation of the hydroxy group of nerol with the carboxy group of acetic acid. This volatile metabolite contributes to the plant's fragrance. Corsican HIEO is characterized by a high level of NA (33.7–38.9%) [3, 7]. No biological activity of NA is described but geranyl acetate, an NA isomer, has antifungal activity [8] and induces potent anticancer effects in Colo-205 colon cancer cells by inducing apoptosis, DNA damage and cell cycle arrest [9].

The *stratum corneum* (SC) provides the body's main barrier to the environment and is key to maintaining optimal cutaneous hydration. The barrier structure of the *stratum corneum* in human skin has four major components: the cornified envelope (CE) and its cytoplasm, the corneocyte lipid envelope (CLE) and its intercellular lipid layer [10]. The formation of the CE is characterized by the expression of a set of genes, such as *loricrin* (LOR), *involucrin* (IVL), *transglutaminase* (TGM1) and *filaggrin* (FLG). IVL is expressed at an early stage of keratinocyte differentiation and promotes CE formation [11]. The most important components of the intercellular lipid layers are ceramides (50%), cholesterol (25%) and free fatty acids (10–20%) [12]. Disturbance in the lipid composition and/or organization is related to changes in the barrier properties and skin diseases (atopic dermatitis, psoriasis...) [13].

The free fatty acids in the SC are predominantly straight chained and dominated by saturated long-chain fatty acids, mainly C24:0 and C26:0 [14]. Cholesterol is the major sterol in the

SC, but cholesterol sulfate is another important skin lipid involved in the keratinocyte differentiation and desquamation process [15].

At least thirteen different subtypes of ceramides are produced in the epidermis, which are composed of long-chain sphingoid bases linked to fatty acid groups (FA) via an amide bond. Among ceramides, the most abundant of these subclasses in the *stratum corneum* are NP, NH, AP and AH mainly with fatty acid chain lengths C24 and C26 and with small contributions from C16 and C18, the latter being the most abundant chain length of sphingoid base [16]. Ceramides constitute a hydrophilic extracellular lipid matrix, indispensable for permeability barrier function, and act as active second messengers, regulating keratinocyte proliferation and differentiation, enhancing proinflammatory cytokine production and modulating immune response [17].

During aging, the skin barrier function is reduced and the composition of the CE changes dramatically due to altered gene coding expression patterns for major components of the CE. There is also an overall reduction in *stratum corneum* lipids and a disturbance in cholesterol and fatty acid synthesis. Cer[EOS] is significantly reduced in seniors (>50 years) compared to younger individuals (20–40 years). Moreover, the degree of fatty acid chain saturation of Cer[EOS], which has marked effects on lamellar and lateral lipid organization, decreases in autumn and winter, partially accounting for worse barrier function. Consequently, there is also evidence of altered permeability barrier to chemical substances and increased transepidermal water flux in aged skin [18].

We previously demonstrated that 24-hour treatment with Corsican HIEO upregulates genes involved in the epidermal differentiation complex (IVL, SPRRs, LCEs, S100-family) in skin explants [19]. NA as a part component of HIEO was tested on skin explants and its activity compared to that of the HIEO containing it. Transcriptomic analysis revealed that 41.5% of HIEO-modulated genes are also regulated by NA; those genes are related to skin barrier formation (keratinocyte differentiation, epidermal differentiation complex and junctions) and ceramide synthesis. We focused on involucrin, which is upregulated at both gene and protein level by treatments. Total lipids and ceramides were also increased, and this was correlated with genes involved in lipid and ceramide synthesis pathways. Those results demonstrated in our experimental conditions that NA mediates the skin barrier formation induced by Corsican HIEO.

Materials and Methods.

Plant material and oil distillation

Aerial parts of *H. italicum* subsp. *italicum* were collected at flowering time in July from a crop cultivation located on the Corsican coast. Fresh aerial parts were hydrodistilled for five hours using a Clevenger-type apparatus.

Gas chromatography–mass spectrometry analyses

Gas chromatography analysis was performed on a gas chromatograph equipped with a flame ionization detector, using a TR-WaxMS-fused silica capillary column (Thermo Fisher Scientific, 60 m x 0.25 mm i.d.; film thickness 0.25 µm). The percentage composition of compounds (relative quantity) in the essential oils was computed from the GC–FID peak areas using the normalization method, without correction factors.

Human skin biopsy collection and treatment

Full-thickness biopsies of abdominal skin, collected during cosmetic surgery, were purchased from suppliers accredited by the French Ministry of Research: Alphenyx (Marseille, France) and DermoBioTec (Lyon, France). The tissue collection used in this study included 3 biopsies of abdominal skin from 33-, 34- and 35-year-old women for histology, microarray analysis, involucrin and lipid staining, and 3 from 36-, 47- and 49-year-old women for ceramide analysis. HIEO and NA were solubilized in DMSO and never exceeded 0.5% in culture medium and was considered as the control. Treatment consisted of 0.1% HIEO or 0.03% NA in the culture medium at day 0 and day 2.

Quadruplicates from each donor were collected 24 hours after treatment for genomic expression analysis and at day 5 for morphological evaluation by histology, IVL detection, lipid and ceramide analysis.

Histological analysis

Explants at day 5 were immediately fixed in neutral buffered formalin 10% (Sigma-Aldrich, Saint-Quentin-Fallavier, France) for 24 hours and embedded in paraffin. Paraffin-embedded formalin-fixed samples were then cut into 5-µm sections and were stained with Masson's trichrome.

Involucrin immunofluorescence, image acquisition and analysis

Labeling was performed on air-dried 5- μm paraffin sections and incubated with anti-involucrin rabbit IgG (6011008, Novocastra). Secondary Alexa Fluor® 488 goat anti-rabbit IgG antibody (Invitrogen, Asnières-sur-Seine, France) was incubated for one hour at room temperature. Nuclear acid counterstaining using DAPI (4',6-diamidino-2-phenylindole) was carried out routinely. As a negative control, primary antibody was replaced by the corresponding control isotype.

Immunofluorescence specimens were visualized using a DMLB Fluorescence Microscope (Leica), and images were captured using a DFC420C digital camera (Leica). Five representative images were captured for each four replicates by condition and eight-bit images were saved. They were processed and analyzed using ImageJ software for microscopy (<http://www.macbiophotonics.ca/imagej/>, Research Service Branch, US National Institutes of Health, United States). The surface area of involucrin immunostainings was measured and the mean of five representative images per replicate was calculated.

Lipid staining

Explants at day 5 were immediately fixed in OCT compound and frozen at -80°C. OCT-fixed samples were then cut into 5- μm sections and after fixation with propylene glycol, skin cryosections were incubated in Oil Red O Solution (Sigma-Aldrich, Saint-Quentin-en-Yvelines, France) for five minutes at room temperature, incubated in Mayer's hematoxylin for one minute, and mounted with coverslip and aqueous mounting medium (Faramount, Dako).

Transcriptome analysis

RNA extraction

For each sample, a small piece of skin (90–100 mg) was disrupted and homogenized using Omni Tissue Homogenizer into TRIzol® reagent. The upper phase was transferred to RNeasy spin columns and total RNA was extracted using mini-RNeasy kits (Qiagen, Courtaboeuf, France) according to the manufacturer's instructions, with the addition of the DNase digestion step. RNA quality/integrity and concentration were assessed using an Agilent 2100 Bioanalyzer (Agilent Technologies, Les Ulis, France) and NanoDrop™ Spectrophotometer (Thermo Fisher Scientific, Asnières-sur-Seine, France), respectively.

Preparation and hybridization of probes

The total RNA (100 ng) of each sample was reverse transcribed, amplified and labeled with Cyanine 3 (Cy3) as instructed by the manufacturer of the One-Color Agilent Low Input Quick Amp Labeling Kit (Agilent Technologies, Les Ulis, France). Cy3-labeled cRNA was hybridized onto Agilent Whole Human Genome Oligo 8X60K V2 Arrays (SurePrint G3 Human Gene Expression 8x60K v2 Microarray Kit, G4851B; 50,599 probes) using reagents supplied in the Agilent Hybridization kit (One-Color Microarray-based Gene Expression Analysis Protocol). The one-color microarray images were extracted with Feature Extraction software (v12.0.0.7), which performs background subtractions and generates a quality control report.

Microarray analysis

Raw data produced from microarrays were imported into GeneSpring GX13.0 software (Agilent) to determine the differentially expressed genes between treated and control samples. The raw data were normalized and filtered by flag using GeneSpring GX13.0 software. The normalization included log₂ transformation, per chip normalization to 75% quantile and dropped per gene normalization to median. Flag filtering included genes that were at least detected in 100 percent of the samples in either condition. In addition, GeneSpring GX13.0 software was used to filter a set of HIEO- or NA-responsive genes for which the expression levels were significantly modified (unpaired moderated t-test, p<0.05), with an average fold change ≥ 2 or ≤ -2 compared to the control group. This result was adjusted for multiple testing by the false discovery rate (FDR) with the Benjamini–Hochberg procedure using a threshold of 0.05. HIEO- or NA-responsive genes were investigated by Ingenuity Pathway Analysis (IPA, Qiagen, Redwood City, CA). Bioinformatic analysis was performed to identify HIEO- or NA-responsive genes. Briefly, outcomes from microarray analysis were first uploaded into Qiagen's IPA system for core analysis and then overlaid with the global molecular network in the Ingenuity Pathway Knowledge Base (IPKB).

QRT-PCR

The reverse transcription reaction was performed on 0.4 µg of RNA template and cDNA was synthesized using an AffinityScript QPCR cDNA Synthesis Kit as instructed by the manufacturer (Agilent Technologies, Les Ulis, France). Quantitative PCR was performed

using optimized TaqMan® gene expression assays (Applied Biosystems) (Table 1) with Brilliant III Ultra-Fast QPCR Master Mix (Agilent Technologies, Les Ulis, France) on the MX3005P Stratagene instrument. Each PCR reaction was done in duplicate. Results were normalized to the expression of the housekeeping genes POLR2A, GAPDH and TBP. qPCR data was analyzed using qBase software (v 2.3) for the management and automated analysis of qPCR data. Expression of target genes was quantified based on the ΔC_q method modified to consider gene-specific amplification efficiencies and multiple reference genes.

Table 1. Primers used for TaqMan Real-time PCR

TaqMan Probe	Assay ID
AQP3	Hs00185020_m1
ABCA12	Hs00292421_m1
CERS3	Hs00698859_m1
ELOVL4	Hs00224122_m1
IVL	Hs00846307_s1
SULT2B1	Hs00190268_m1
TGM1	Hs00165929_m1
UGCG	Hs00916612_m1
GAPDH	Hs99999905_m1
HPRT1	Hs99999909_m1
POLR2A	Hs00172187_m1
TBP	Hs00427620_m1

Ceramide extraction and analysis

Ceramide content in the epidermis were extracted from tissues by a dual liquid–solid extraction method. The lipid solution was then completely dried under N₂ at 30°C. Residues were re-suspended in 50 µl of a chloroform/methanol mixture. Ceramides were analyzed by a LC/MS Ultimate 3000 liquid chromatography system coupled to a MSQ Plus single quadrupole mass spectrometer (Thermo Fisher Scientific, Sunnyvale, CA).

Results

HIEO composition

Overall, 15 components were identified, accounting for 83.12% of the complete essential oil composition (Table 2). Oxygenated monoterpenes were the most abundant chemical class of compounds with 43.76% of the total content. NA showed the largest relative abundance, accounting for 32.80% of the total, followed by neryl propionate (4.66%), linalool and italicene (4.29%) and nerol (2.01%) for this chemical class. The sesquiterpene hydrocarbons showed a relative abundance of 15.53% with γ -curcumene (12.31%), followed by α -curcumene (2.59%) and α -cedrene (0.63%). Ketones represented by Italidiones I and II accounted for 10.34%. Hydrocarbon monoterpenes were less abundant (7.53%) with limonene (4.83%), α -pinene (2.02%) and β -pinene (0.68%). Sesquiterpene alcohols were represented by β -eudesmol (3.57%) and ether monoterpenes by 1,8-cineole (0.82%).

Table 2. Chemical composition of HIEO from Corsica

N°	Tr (min) ^a	Compound	Percentage
1	8.50	α -pinene	2.02
2	10.98	β -pinene	0.68
3	14.60	Limonene	4.83
4	14.99	1,8-cineol	0.82
5	30.68	α -cedrene	0.63
6	33.30	Linalool + italicene	4.29
7	36.30	β -caryophyllene	1.57
8	41.80	γ -curcumene	12.31
9	43.77	Neryl acetate	32.80
10	46.08	α -curcumene	2.59
11	46.95	Neryl propionate	4.66
12	47.22	Nerol	2.01
13	51.94	Italidiones 1 and 2	10.34
15	63.21	β -eudesmol	3.57

^a: Retention time (min) of corresponding constituent obtained by GC-FID,
Percentage = relative abundance

NA drives 41.5% of HIEO gene regulation

We performed a transcriptome analysis using Agilent Whole Human Genome Oligo Microarrays 8x60K V2 on skin explant from three age-related donors (34 ± 1 years old) treated with HIEO (0.1%) or NA (0.03%), representing the percentage of NA found in HIEO (30%), and experiments were carried out independently in quadruplicate. A two-fold change threshold together with a *p*-value of 0.05 was used to identify differentially expressed probe sets. Fig 1 depicts the numbers and overlap in differentially expressed genes (≥ 2.0 -fold, unpaired t-test $p < 0.05$) in skin explant following HIEO or NA exposure. The Venn diagram illustrated that HIEO and NA have 1,280 common probe sets, indicating that 41.5% of transcripts regulated by HIEO treatment were also regulated by NA.

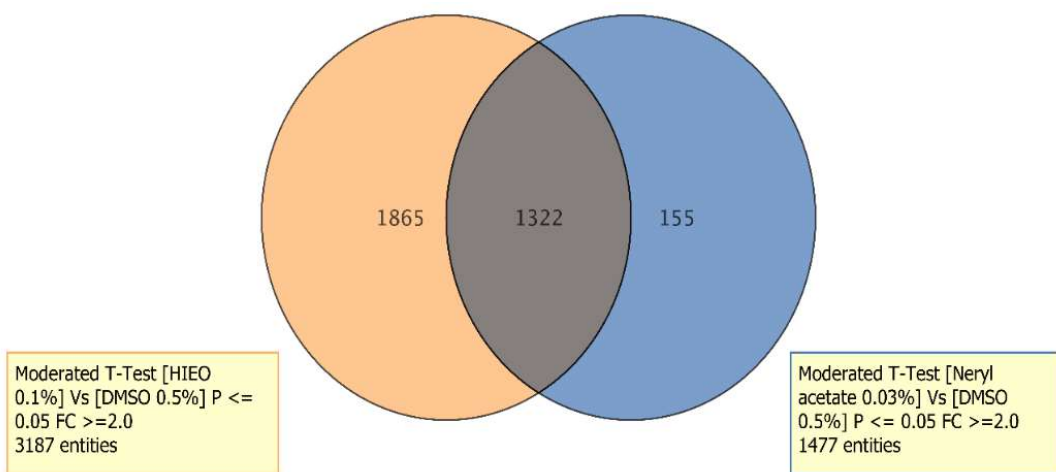


Fig 1. HIEO and NA share 1,322 regulated transcripts

Venn diagram showing the number of similarly and differentially regulated genes between HIEO and NA treatment. Numbers in no overlapping sections represent genes unique to HIEO or NA conditions, while numbers in overlapping areas represent genes shared by HIEO or NA conditions.

The 1,322 probe sets were scrutinized with IPA (Qiagen, Redwood City, CA, USA), which highlighted 1,204 analysis-ready molecules and revealed the activation z-score of the pathway identified as “skin differentiation” to be equal to 2.3. When the activation z-score is superior to 2, it predicts the activation states of the defined biological function. All these results strongly suggest that NA and HIEO induce skin differentiation. Fig 2, which details

this pathway, shows that genes involved in the function are related to skin barrier formation, keratinocyte differentiation and ceramide synthesis.

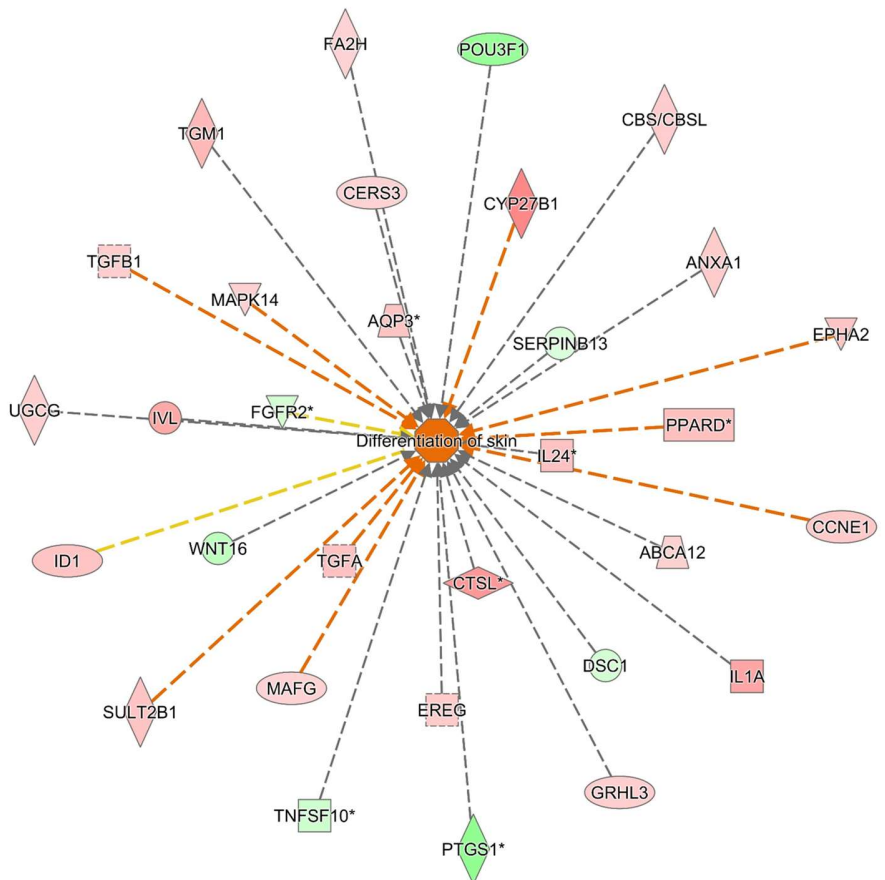


Fig 2. Biological Function Analysis using IPA predicts activation of skin differentiation from differentially expressed genes shared by neryl acetate and HIEO conditions (*p*-value: <0.05, Z-score: 2.). Fig 2 represents genes associated with the biological function “skin differentiation” which are altered in the uploaded dataset. Genes that are upregulated are displayed within red nodes and those downregulated are displayed within green nodes. The intensity of color in a node indicates the degree of up-(red) or down-(green) regulation. An orange line indicates predicted upregulation, whereas a blue line indicates predicted downregulation. A yellow line indicates expression being contradictory to the prediction. A gray line indicates that direction of change is not predicted. Solid or broken edges indicate direct or indirect relationships, respectively.

To validate genes identified by microarrays, we selected eight upregulated genes (ABCA12, AQP3, CERS3, ELOVL4, IVL, SULT2B1, TGM1 and UGCG) for qPCR confirmation. Data were presented as fold changes in gene expression normalized to four housekeeping genes

(GAPDH, HPTR1, POLR2A, TBP) and relative to the DMSO control sample. qPCR analysis (independent RNA extractions from biological replicates used for microarray analysis) confirmed the direction of change detected by microarray analysis (Fig 3). This correlation indicated the reliability of microarray results. The primers used in the qPCR analysis are shown in Table 1.

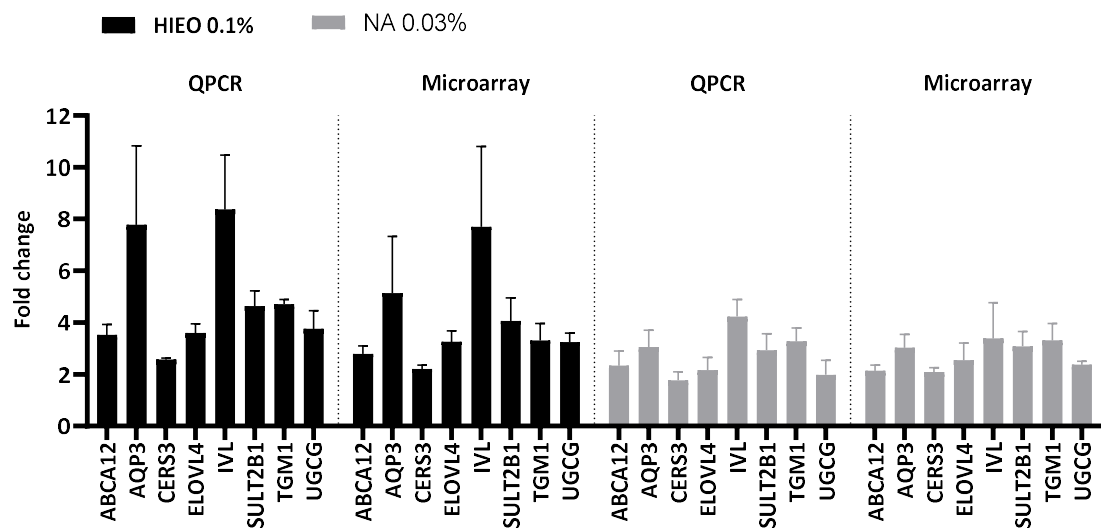


Fig 3 QRT-PCR confirms HIEO and NA changes identified in microarray expression data

Results indicate relative gene expressions of HIEO- (0.1%) or NA-treated skin (0.03%) compared to the control DMSO (0.5%). QRT-PCR results for a subset of genes identified as skin barrier (AQP3, IVL, TGM1) and ceramide biosynthesis (ABCA12, CERS3, ELOVL4, SULT2B1, UGCG) validated the microarray expression data for skin explants. Data are the mean ± standard error of quadruplicate explant for each donor from three distinct donors.

NA increases formation of the skin barrier

The epidermal differentiation in the presence of NA or HIEO is favored by the upregulation or downregulation of certain genes. They are either involved in mechanisms leading the differentiation/proliferation of keratinocytes or are markers of a differentiated state. As shown in Figure 4A, CBS/CBSL, CCNE1, GRHL3, EPHA2, CSTL, PPAR δ and RRAS2, which are involved in the differentiation process, were upregulated while PTGS1 and POU3F1, two differentiation repressors, were downregulated. VAV3 and WNT16, which regulate proliferation, decreased (Fig 4A).

In parallel, KRT14 expressed in the basal layer of the epidermis and its partner KRT5 were downregulated by both treatments. KRT10 and KRT1 expressed in the differentiated suprabasal cells were also downregulated. Those keratins move upwards to form the granular layer during terminal differentiation and their expressions cease with the induction of late differentiation markers such as IVL, which was upregulated by NA and HIEO treatment. SPRR3 and CRNN, other genes of the epidermal differentiation complex (EDC), and AQP3 and TGM1, involved in terminal differentiation of the epidermis, were upregulated while LCE2A, another EDC gene, was downregulated by NA and HIEO treatment (Fig 4B).

Intercellular junctions were also upregulated with genes related to gap junctions (GBJ3, PANX2), tight junctions (CLDN7) and desmosomes (DSG3, PKP2) (Fig 4C).

The growth factors upregulated in our study included cell proliferation and/or migration regulators such as members of the EGF family (HBEGF, EREG, AREG, EPGN) but two of their receptors, FGFR2/FGFR3, were downregulated by NA and HIEO treatment (Fig 4D).

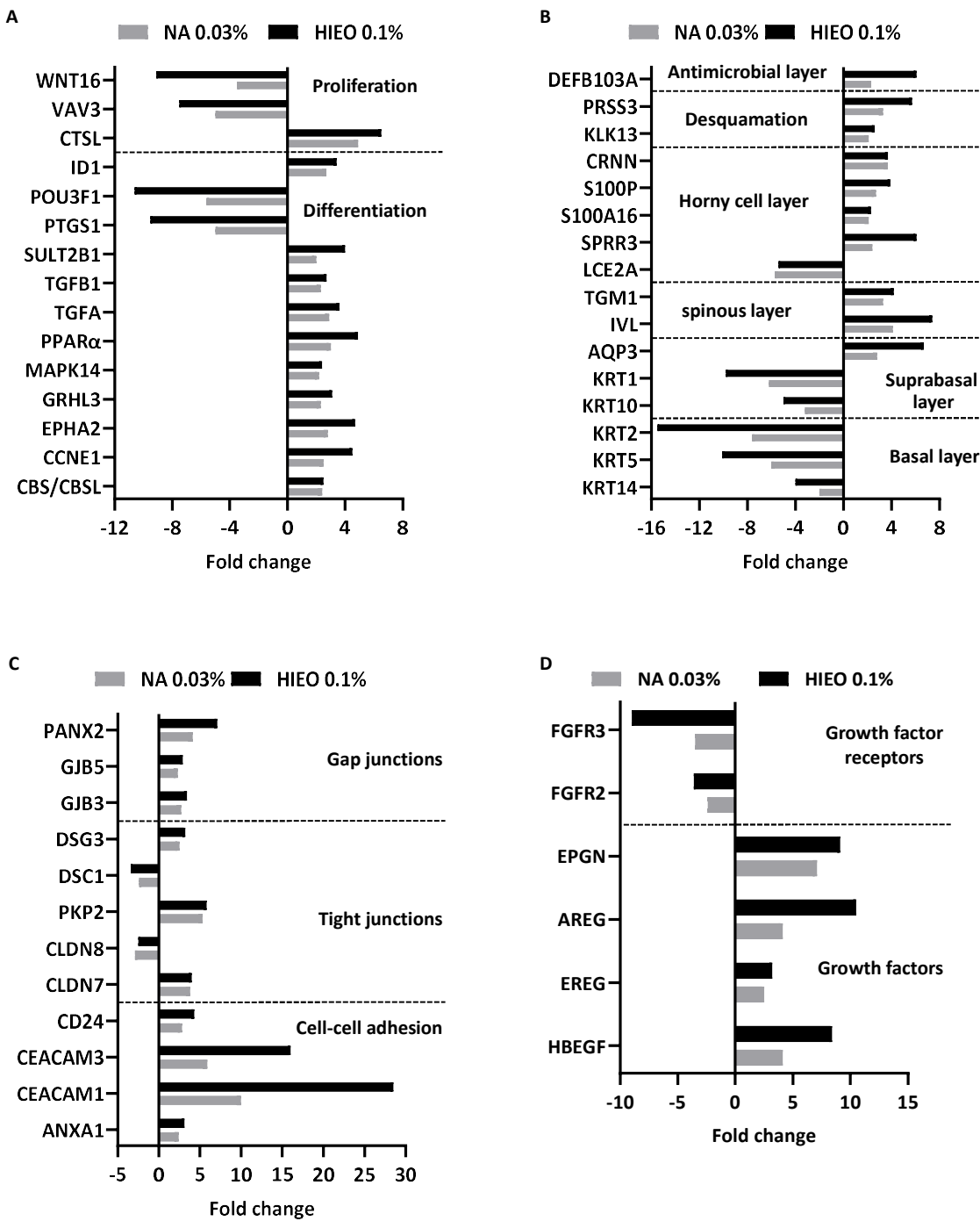


Fig 4. NA increased the genes involved in barrier formation and its reinforcement. **A:** Genes involved in the differentiation and proliferation of keratinocytes. **B:** Genes involved in the structure of the epidermis. **C:** Genes involved in cellular junctions. **D:** Genes of growth factors and their receptors. Mean fold-change induced by HIEO and NA in quadruplicate explant for each donor from three distinct donors after 24-hour treatment are shown.

NA increases involucrin protein

Fig 5A compares the morphology of the explant at day 5 between 0.5% DMSO, 0.1% HIEO or 0.03% NA. There are no discernible tissue structure alterations following treatment.

Immunohistochemical staining confirmed an increased expression of involucrin protein in HIEO- and NA-treated skin. Involucrin staining is increased in spinous layer following treatment with HIEO or NA (Fig 5B). Protein quantification by image analysis (Fig 5C) confirmed a significant increase in involucrin area related to the epidermis area for both HIEO and NA treatment. HIEO led to a more pronounced increase in expressions of involucrin protein ($+111 \pm 37\%$) than NA ($+51 \pm 18\%$) compared to the control DMSO 0.5%.

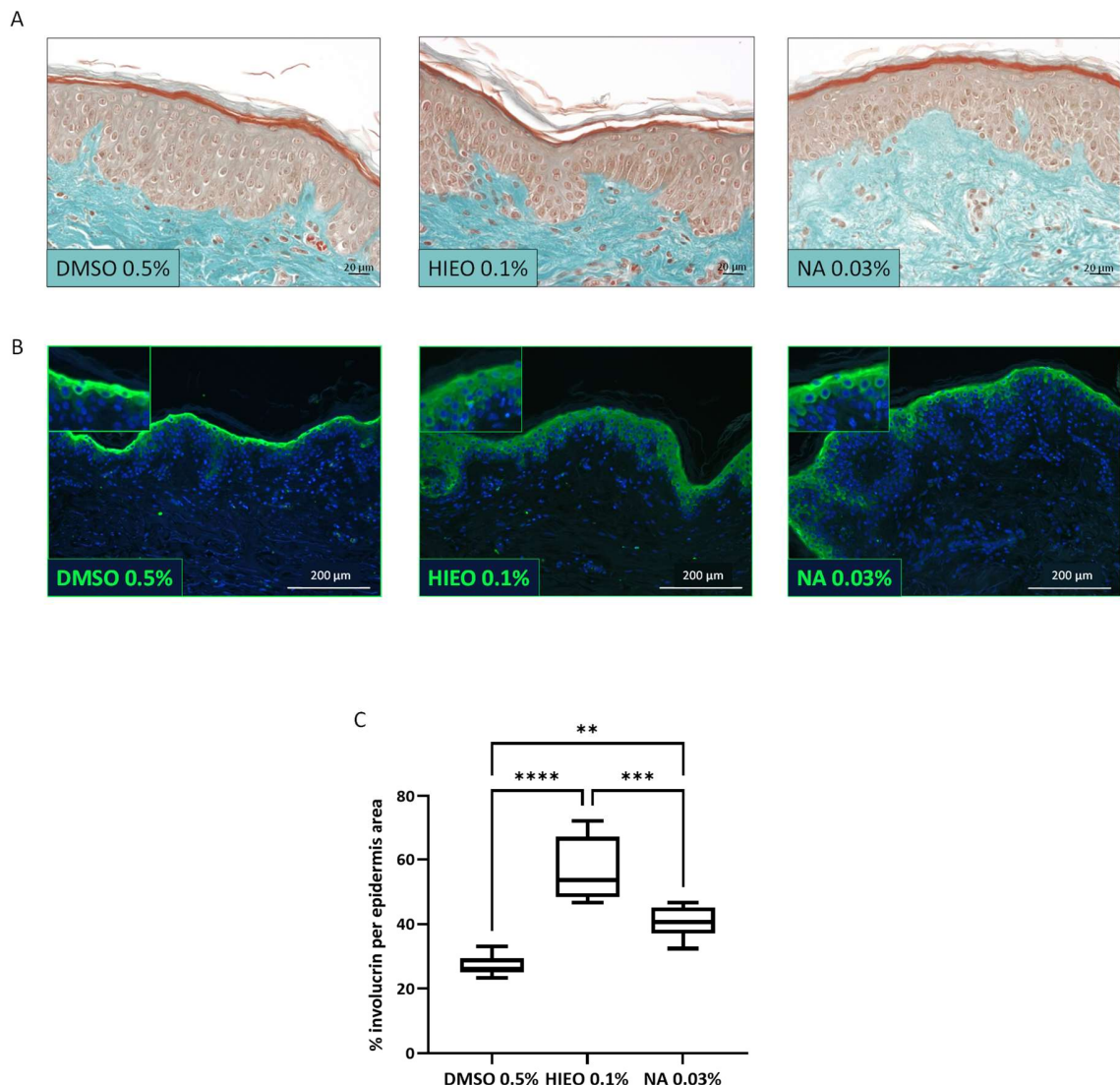


Fig 5. NA increased involucrin protein

A: Histological and morphological analysis at day 5 using Masson's trichrome staining after application of DMSO 0.5%, HIEO 0.1% or NA 0.03%. Scale bar, 20 μ m. **B:** Confocal microscopy observation of involucrin immunostaining. Scale bare, 200 μ m. Involucrin in green, nuclei in blue. **C:** Quantification of involucrin surface area by image analysis. Data are expressed in % involucrin per epidermis area. Involucrin data are presented as box and whisker plot where boxes span first and third quartiles, bars as the median values, and whiskers as the minimum and maximum mean of five representative images per replicate (n=4). **p<0.01; ***p<0.001; ****p<0.0001 (Mann–Whitney test).

NA induces ceramide biosynthesis: Transcriptomic analysis

As shown in Fig 6, genes involved in all steps of the acylglycosylceramide biosynthesis were induced after 24 hours of NA and HIEO treatment.

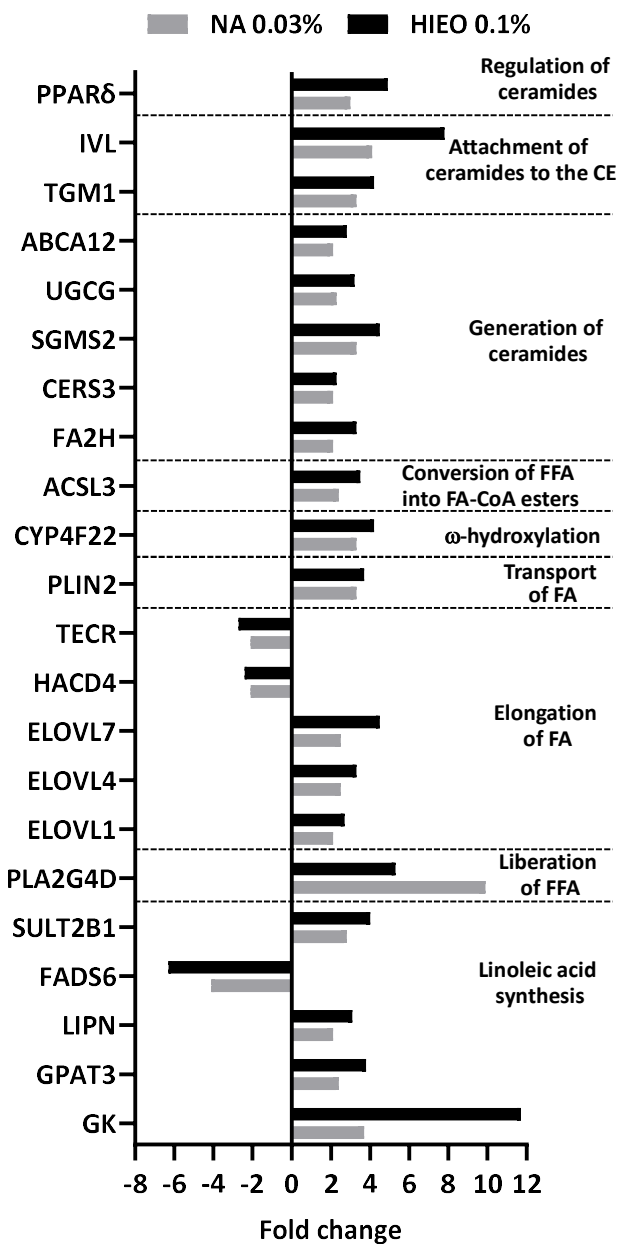


Fig 6. NA increased the gene expression of ceramide synthesis-related enzymes

Genes of enzymes involved in linoleic acid synthesis, fatty acid (FA) elongation, ω-hydroxyceramide production and ceramide generation were analyzed. Mean fold-changes induced by HIEO and NA (NA) in quadruplicate explant for each donor from three distinct donors after 24-hour treatment are shown.

NA increases total lipid production

A general examination of lipid production using Oil Red O was performed (Fig 7). This staining indicates that NA and HIEO increased the incorporation of lipids into the intercellular space of the epidermis compared to the control DMSO 0.5%.

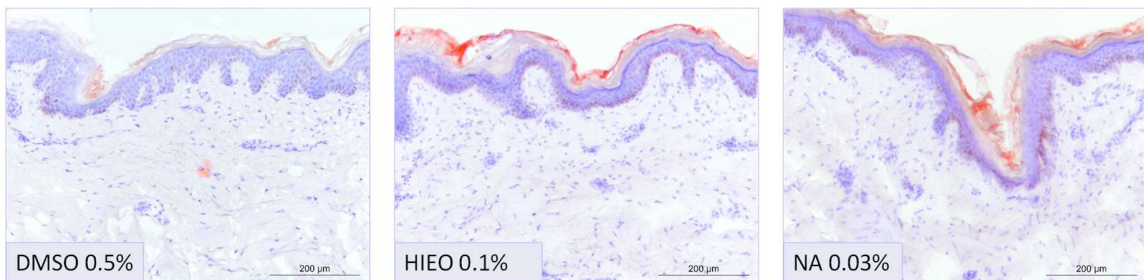


Fig 7. NA increased lipids in the epidermis

Skin sections were stained with Oil Red O to detect lipid in the epidermis at day 5 after DMSO 0.5%, NA 0.03% or HIEO 0.1% treatment. Optical representative images show the location of dye in the intercellular spaces of the epidermis. Lipids are stained in red. Scale bar, 200 μ m.

NA increases ceramide content in the epidermis

Using LC/MS, we measured CER[NS] and CER[AS] in the epidermis of skin explants ($n=3$) from three female donors (age range 36 to 49 years) treated with DMSO (0.5%) as the control, NA (0.03%) or HIEO (0.1%) for five days.

As shown in Fig 8, the increase in total ceramides was significantly higher in the presence of HIEO (0.1%) than NA (0.03%), ranging from +114.2% to +64.2% compared to DMSO 0.5%. 6 CER[NS] and 2 CER[AS] were identified and revealed that the treatment with NA or HIEO elicited a significant increase in almost all ceramides detected except CER[N(24:1)S(18)], which is decreased by both treatments. A significant difference was found for CER[N(16)S(18)], CER[N(18)S(18)] and CER[(14:1)S(18)] between HIEO and NA treatment. No difference was observed for CER[A(16)S(18)], CER[N(20)S(18)], CER[A(24)S(18)], CER[N(24)S(18)] and CER[N(26)S(18)] with either treatment.

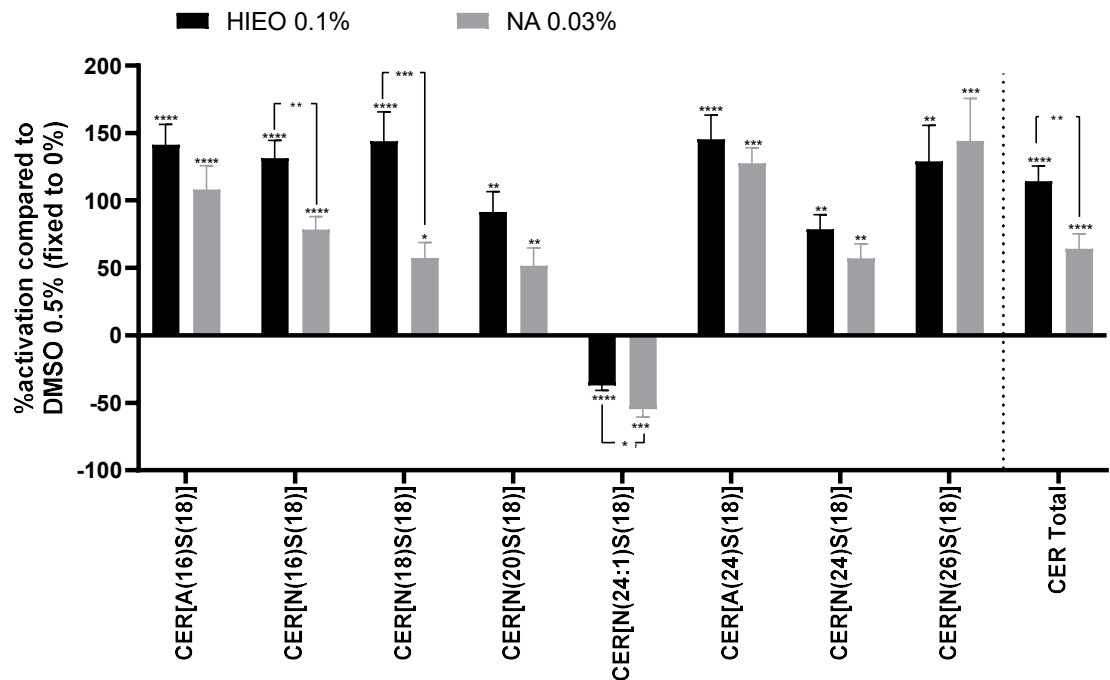


Fig 8. NA increased Ceramides in the epidermis

Ceramides were extracted from epidermis and subjected to LC/MS for determining the levels of each ceramide species. Data are the mean triplicate explants for each donor (n=3) related to DMSO, fixed to 0%. *p<0.05; **p<0.01; ***p<0.001; ****p<0.0001 (One-way Anova with post-hoc Tukey HSD test).

Discussion

The chemical composition of the tested HIEO in our study is characteristic of Corsican HIEO, with NA (32.80%) as the major compound and a low concentration in α -pinene (2.02%) [7]. We previously demonstrated that Corsican HIEO effectively promotes skin barrier function and hydration [19].

Because NA is the major compound of HIEO from Corsica with unknown skin activity, we wanted to elucidate its role in the biological functions of HIEO. For that, we compared their biological activity by transcriptomic analysis; NA was tested at a dose equivalent to that found in Corsican HIEO. We discovered that HIEO and NA share 1,322 common probe sets and 41.5% of HIEO-regulated transcripts were due to NA, with genes involved in skin barrier formation, keratinocyte differentiation and ceramide synthesis.

The predominant problem with aging skin is a disturbed barrier function characterized by dryness, reduced immune response and slow wound healing [20]. The skin's primary function is to act as a protective barrier between the organism and its external environment, minimizing water loss from the body whilst preventing the entry of pathogens and allergens. Epidermal barrier dysfunction can exacerbate sensitive skin conditions, dryness and infections.

The analysis of regulated gene expression suggests that NA drives at least and HIEO have a significant effect on the keratinocyte differentiation process and promote skin barrier formation. Indeed, genes that code for protein-regulating differentiation are upregulated, with increased IVL expression at mRNA and protein level. This protein is incorporated as a component of the cornified envelope [21] via the TGM1 action that is also increased by NA and HIEO treatment. By increasing IVL and TGM1, NA and HIEO contribute to barrier maintenance, and with the upregulation of AQP3, NA and HIEO should facilitate osmotically driven transport of the water and glycerol.

Lipids are important constituents of the human epidermis. Either free and organized into broad lipid bilayers in the intercorneocyte spaces, or covalently bound to the corneocyte envelope, they play a crucial role in permeability barrier function as a blocker of transepidermal water loss. In aged skin, biochemical analysis of epidermal lipids reveals that

the content of three major lipid species — ceramide, cholesterol and fatty acids — was reduced [18]. This could be explained by the reduced activity of each lipid's rate-limiting enzymes. By increasing lipid production, the application of HIEO or NA could reinforce barrier function, increase water retention and lower penetration of exogenous compounds.

Ceramides are sphingolipids that consist of a long chain of sphingosine base linked to long-chain fatty acid via an amide bond. In this study, we focused on the more common 18-carbon sphingosine base, the most abundant sphingoid base in the epidermis and known to promote keratinocyte differentiation [17] and non-hydroxylated (N) and hydroxylated (A) medium-chain ceramides that represent around 21 species. NA and HIEO increased the production of non-hydroxylated CER[N(20)S(18)], CER[N(24)S(18)] and CER[N(26)S(18)] or hydroxylated CER[A(24)S(18)] at similar levels. This production can be attributed to the increasing expression of ELOVL1 and ELOVL4 [22] induced by HIEO and NA treatment. Ceramides with small-chain non-hydroxy and hydroxy fatty acid (16–18 carbons) were more strongly increased by HIEO than NA, probably correlated to the expression of ELOVL7 (C16 to C20-CoAs) [23] also rising more with HIEO than NA. Acyl-ceramides (EOS, EOH, EOP and EODS), which account for 12% of *stratum corneum* ceramides, were not evaluated by LC/MS analysis in this study. However, protein transcripts involved in the four steps of acyl-ceramide production were upregulated by NA and HIEO.

Conclusion.

Our results demonstrate that NA, the major component of HIEO, strengthens the skin barrier function by increasing lipid and ceramide content in the SC through enhancing the expressions of ceramide synthesis-related enzymes required for the glucosylceramide pathway. Furthermore, both compounds increase the epidermal differentiation complex by stimulating the expression of IVL (transcript and protein). In addition, we demonstrate for the first time that HIEO-regulated effects in this study are mediated by its principal component, NA. Therefore, we anticipate that NA, the major component of Corsican HIEO, may be effective in improving skin barrier function and moisture retention in age-associated skin conditions.

Acknowledgments. Laboratoires M&L SA - Groupe L'Occitane funded the study.

Conflict of Interest Statement. NONE.

References.

1. Antunes Viegas D, Palmeira-de-Oliveira A, Salgueiro L, Martinez-de-Oliveira J, Palmeira-de-Oliveira R (2014) *Helichrysum italicum*: from traditional use to scientific data. *J Ethnopharmacol* 151:54–65.
2. Leonardi M, Ambrysiewska KE, Melai B, Flamini G, Cioni PL, Parri F, Pistelli L (2013) Essential-oil composition of *Helichrysum italicum* (Roth) G. Don ssp. italicum from Elba Island (Tuscany, Italy). *Chem Biodivers* 10:343–355.
3. Bianchini A, Tomi P, Costa J, Bernardini AF (2001) Composition of *Helichrysum italicum* (Roth) G. Don fil. subsp. italicum essential oils from Corsica (France). *Flav Fragrance J* 16:30–34.
4. Morone-Fortunato I, Montemurro C, Ruta C, Perrini R, Sabetta W, Blanco A, Lorusso E, Avato P (2010) Essential oils, genetic relationships and *in vitro* establishment of *Helichrysum italicum* (Roth) G. Don ssp. italicum from wild Mediterranean germplasm. *Ind Crops Prod* 32:639–649.
5. Schipilliti L, Bonaccorsi IL, Ragusa S, Cotroneo A, Dugo P (2016) *Helichrysum italicum* (Roth) G. Don fil. subsp. italicum oil analysis by gas chromatography – carbon isotope ratio mass spectrometry (GC-CIRMS): a rapid method of genotype differentiation? *J Ess Oil Res* 28:1-9.
6. Bianchini A, Santoni F, Paolini J, Bernardini AF, Mouillet D, Costa J (2009) Partitioning the relative contributions of inorganic plant composition and soil characteristics to the quality of *Helichrysum italicum* subsp. italicum (Roth) G. Don fil. Essential oil. *Chem. Biodivers* 6:1014–1033.
7. Bianchini A, Tomi P, Bernardini AF, Morelli I, Flamini G, Cioni PL, Usaï M, Marchetti M (2003) A comparative study of volatile constituents of two *Helichrysum italicum* (Roth) Guss. Don Fil subspecies growing in Corsica (France), Tuscany and Sardinia (Italy). *Flav Fragrance J* 18:487–491.
8. Khayyat SA, Sameeh MY (2018) Bioactive epoxides and hydroperoxides derived from naturally monoterpenes geranyl acetate. *Saudi Pharm J*. 26:14-19.
9. Qi F, Yan Q, Zheng Z, Liu J, Chen Y, Zhang G (2018) Geraniol and geranyl acetate induce potent anticancer effects in colon cancer Colo-205 cells by inducing apoptosis, DNA damage and cell cycle arrest. *J BUON*. 23:346-352.

10. Elias PM, Gruber R, Crumrine D, Menon G, Williams ML, Wakefield JS, Holleran WM, Uchida Y (2014) Formation and functions of the corneocyte lipid envelope (CLE). *Biochim Biophys Acta* 1841:314-318.
11. Candi E, Schmidt R, Melino G (2005) The cornified envelope: A model of cell death in the skin. *Nat Rev Mol Cell Biol* 6:328.
12. van Smeden J, Janssens M, Gooris GS, Bouwstra JA. The important role of stratum corneum lipids for the cutaneous barrier function. *Biochim Biophys Acta*. 2014;1841: 295–313.
13. Coderch L, Lopez O, de la Maza A, Parra JL (2003) Ceramides and skin function. *Am J Clin Dermatol* 4:107–129.
14. Uchiyama M, Oguri M, Mojumdar EH, Gooris GS, Bouwstra JA (2016) Free fatty acids chain length distribution affects the permeability of skin lipid model membranes. *Biochim Biophys Acta* 1858:2050–2059.
15. Elias PM, Williams ML, Choi EH, Feingold KR (2014) Role of cholesterol sulfate in epidermal structure and function: lessons from X-linked ichthyosis. *Biochim Biophys Acta* 1841:353–361.
16. Pruett ST, Bushnev A, Hagedorn K, Adiga M, Haynes CA, Sullards MC, Liotta DC, Merrill AH Jr (2008) Biodiversity of sphingoid bases ("sphingosines") and related amino alcohols. *J Lipid Res* 49:1621-1639
17. Paragh G, Schling P, Ugocsai P, Kel AE, Liebisch G, Heimerl S, Moehle C, Schiemann Y, Wegmann M, Farwick M, Wikonkál NM, Mandl J, Langmann T, Schmitz G (2008) Novel sphingolipid derivatives promote keratinocyte differentiation. *Exp Dermatol* 17:1004-1016
18. Ghadially R, Brown BE, Sequeira-Martin SM, Feingold KR, Elias PM (1995) The aged epidermal permeability barrier. Structural, functional, and lipid biochemical abnormalities in humans and a senescent murine model. *J Clin Invest* 95:2281–2290.
19. Lemaire G, Lemaire V, Olivero M, Dugas E, Devilard E (2016) Geographical link to efficiency of *Helichrysum italicum*. *Personal Care Magazine*. 2:23-25.
20. Robert L, Labat-Robert J, Robert AM (2009) Physiology of skin aging. *Pathol Biol (Paris)* 57:336-341.

21. Eckert RL, Yaffe MB, Crish JF, Murthy S, Rorke EA, Welter JF. Involucrin--structure and role in envelope assembly. *J Invest Dermatol.* 1993;100: 613-617
22. Ohno Y, Nakamichi S, Ohkuni A, Kamiyama N, Naoe A, Tsujimura H, Yokose U, Sugiura K, Ishikawa J, Akiyama M, Kihara A (2015) Essential role of the cytochrome P450 CYP4F22 in the production of acylceramide, the key lipid for skin permeability barrier formation. *Proc Natl Acad Sci USA.* 112:7707-7712.
23. Nie L, Pascoa TC, Pike ACW, Bushell SR, Quigley A, Ruda GF, Chu A, Cole V, Speedman D, Moreira T, Shrestha L, Mukhopadhyay SMM, Burgess-Brown NA, Love JD, Brennan PE, Carpenter EP (2021) The structural basis of fatty acid elongation by the ELOVL elongases. *Nat Struct Mol Biol* 28:512-520.